Economic viability and CO2 emissions of hydrogen production for ammonia synthesis: A comparative analysis across Europe

Advances in Applied Energy 17 (2025) 100204

Contents lists available at ScienceDirect

Advances in Applied Energy

journal homepage: www.elsevier.com/locate/adapen

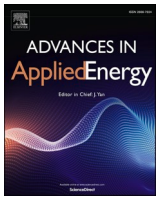

Economic viability and CO_2 emissions of hydrogen production for ammonia synthesis: A comparative analysis across Europe

Alessandro Magnino *, Paolo Marocco, Massimo Santarelli, Marta Gandiglio

Department of Energy, Politecnico di Torino, Corso Duca degli Abruzzi 24, 10129 Torino, Italy

ARTICLE INFO

Keywords:
Ammonia
Levelised Cost Of Ammonia
Water electrolysis
Steam Methane Reforming
Decarbonisation

ABSTRACT

Ammonia production accounts for 15–20% of greenhouse gas emissions from the chemical sector. Traditionally, ammonia is produced via Steam Methane Reforming (SMR) for hydrogen production, coupled with the Haber-Bosch process. This study compares the SMR-based configuration with emerging alternatives based on water electrolysis – Proton Exchange Membrane Electrolyser Cell (PEMEC) and Solid Oxide Electrolyser Cell (SOEC) – from both economic and CO_2 emissions perspective. Process models for the three plant layouts are developed, incorporating heat integration between different components. The economic results are presented in terms of the levelised cost of ammonia, which accounts for both capital and operating expenses over the plant's lifetime. Sensitivity analyses on electricity and methane prices are conducted to assess the cost-competitiveness of each technology across various scenarios. The outcomes reveal that the optimal technology is highly dependent on electricity prices. PEMEC systems are the most cost-effective option at very low electricity prices (approximately 0.02 €/kWh_e), while SOEC systems become more competitive as prices rise due to their higher efficiency. Above 0.08 €/kWh_e, SMR emerges as the most viable option. Special attention is given to the CO_2 emissions from both SMR and electrolyser systems, also considering the carbon intensity of the electricity used. While electrolysis is often assumed to be carbon-free, this research shows that electrolysers can produce more emissions than SMR, depending on the electricity carbon intensity: when carbon intensity exceeds about 260 gCO_2/kWh_e, SMR results in lower emissions than the electrolyser-based pathways. Finally, future projections suggest that SOEC technology will become highly cost-competitive by 2030–2040.

1. Introduction

To reach the target set in the Paris Agreement of limiting global warming to 1.5°C above pre-industrial levels [1], a rapid reduction in Greenhouse Gas (GHG) emissions is necessary. In particular, the goal of achieving global net-zero carbon dioxide (CO_2) emissions [2] is still a distant goal. Strong decarbonisation of many hard-to-abate sectors is required, moving from traditional fossil-based processes to less impactful alternatives.

Ammonia (NH_3) production is a major contributor to GHG emissions, currently accounting for about 1% of global CO_2 emissions and 15–20% of the emissions associated with the chemical sector [3]. Most of these emissions are linked to hydrogen (H_2) production, upstream of ammonia synthesis, which is currently generally based on Steam Methane Reforming (SMR) [4]. Ammonia is mainly used as a precursor for many nitrogen fertilisers, and it is estimated that food provision for half of the global population heavily depends on synthetic fertilisers derived from ammonia [5]. With the anticipated population growth and the consequent rise in food demand, the global demand for ammonia (>150 Mt in 2023 [6]) is also expected to increase [7], as showed in Fig. 1b. Besides its extensive use in the agricultural sector, ammonia is also widely used in the production of explosives, plastics, polymers and acids. Additionally, there is growing interest in using ammonia as a fuel for internal combustion engines [8], gas turbines [9] and fuel cells [10]. This interest is driven by several factors: ammonia has a lower heating value of 5.22 kWh/kg [11], its combustion produces no CO_2 emissions, and it can be stored and transported relatively easily and cheaply [12], either in liquid form via compression (8 bar and ambient temperature) or via cryogenics (−33°C and atmospheric pressure) [13].

Although some pioneering studies investigated the possibility of producing ammonia through direct electroreduction of nitrogen [15–17], the only method for ammonia production currently exploited

* Correspondence author at: Department of Energy, Politecnico di Torino, Corso Duca degli Abruzzi 24, 10129 Torino, Italy
E-mail addresses: alessandro.magnino@polito.it (A. Magnino), paolo.marocco@polito.it (P. Marocco), massimo.santarelli@polito.it (M. Santarelli), marta.gandiglio@polito.it (M. Gandiglio).

https://doi.org/10.1016/j.adapen.2024.100204
Received 27 August 2024; Received in revised form 13 December 2024; Accepted 17 December 2024
Available online 21 December 2024

at industrial scale is the Haber-Bosch (HB) process. According to IEA [14], in 2020 almost 100% of hydrogen used for NH_3 synthesis was produced from fossil sources: mostly Natural Gas (NG) (72%) (grey ammonia in case carbon capture is not present, blue ammonia if CO_2 capture is included [18]) and coal (26%) (see Fig. 1a). Hydrogen generated from water electrolysis accounted for <1 % of the total. To reduce the environmental impact of ammonia production, it is crucial to increase this percentage, as water electrolysis not only avoids the exploitation of finite fossil resources, but also allows for the effective use of renewable energy sources [19], potentially producing carbon-free hydrogen. Among the electrochemical pathways for H_2 production, most promising alternatives are today represented by Proton Exchange Membrane Electrolyser Cells (PEMECs) and Solid Oxide Electrolyser Cells (SOECs). Important differences between these two technologies include their operating temperature, current costs and energy consumption. SOEC systems indeed operate at high temperatures and generally have higher investment costs, but they offer greater cell efficiency [20]. On the other hand, PEMEC systems operate at lower temperatures and have lower investment costs due to their wider diffusion and maturity. While PEMEC systems generally require low or null pre-heating of the inlet flows, key issue connected to the SOEC technology is the heat required for water pre-conditioning. Indeed, inflow water must pass through a steam generator and an additional heater to reach the stack operating temperature, to avoid damages from temperature gradients inside the cell. If the needed thermal energy has to be provided from auxiliary systems (electric heaters or gas burners), the energy consumption of the SOEC systems results to be very high, often becoming less efficient than the alternative PEMEC-based solution [21]. This issue can be mitigated by coupling the electrolyser with the HB reactor, which is highly exothermic: reusing the waste heat from the HB process can strongly reduce the energy demand of the auxiliary systems in the SOEC. Similar considerations apply to the SMR process as it also requires high operating temperatures, and the thermal needs of the auxiliary systems can have a significant impact [22].

To properly compare competing solutions, the Levelised Cost Of Ammonia (LCOA) is generally used in the literature. This parameter provides a clear view of ammonia production costs, facilitating a quick evaluation of the competitiveness of the different alternatives. Nami *et al.* [23] compared alkaline electrolysers (AEC) and SOECs with grey and blue ammonia under different scenarios from an economic perspective. They concluded that currently the LCOA is about 700 and 950 €/tNH_3 (135 and 183 €/MWh) for the AEC and SOEC pathways, respectively. However, their study did not include evaluations on the emissions connected to ammonia produced via water electrolysis. Mersch *et al.* [24] conducted a similar comparison among grey, blue and PEMEC-produced ammonia. In addition to assessing the LCOA for the different configurations, they also evaluated the CO_2 emissions associated with ammonia production depending on the carbon intensity of the grid electricity. The resulting LCOA values, reported as a function of the electricity and methane prices, ranged between 200 and 1400 USD/tNH_3 (38 and 271 USD/MWh). Zhang et al. [25] analysed ammonia production through SMR, biomass-to-ammonia pathway and SOEC. They found that, at current costs, ammonia produced via SOEC is considerably more expensive than that from SMR (666 vs 387 USD/tNH_3, i.e., 129 vs 75 USD/MWh). Campion *et al.* [26] explored the LCOA resulting from plants using AECs or SOECs in various locations; depending on the characteristics of the site, electricity was supplied through different combinations of wind, photovoltaic panels and grid. The LCOA ranged from 750 to 1400 €/tNH_3 (145 to 271 €/MWh), with the most cost-effective solutions achieved using AECs. Sousa *et al.* [27] developed a model of an ammonia production plant including a PEMEC system and assumed carbon-free electricity from a hydropower plant. They investigated the LCOA under varying electricity prices: currently, the LCOA ranges from 750 to 1500 €/tNH_3 (145 to 290 €/MWh), depending on electricity prices that vary from 0 to 0.06 €/kWh. Kakavand *et al.* [28] analysed different plants based on PEMEC and located in different regions of Iran, exploiting solar and wind resources. Their findings indicated that the costs for ammonia production range between 580 and 1000 USD/tNH_3 (112 and 193 USD/MWh). Lee et al. [29] examined three different electrolyser technologies (AEC, PEMEC and SOEC) from an economic perspective. They concluded that AEC is generally the most cost-effective solution, with costs reaching 1000–1100 USD/tNH_3 (193–213 USD/MWh) with an electricity price of 0.06 USD/kWh. However, their work did not include any evaluation on the carbon intensity of the processes. A study by Bicer *et al.* [30] focused on the life cycle assessment of nuclear-based hydrogen and ammonia production methods and compared their environmental impacts with conventional steam methane reforming pathways. However, they did not specifically address the LCOA calculation. Egerer *et al.* [31] computed the LCOA for green (employing PEMEC and AEC), blue and grey ammonia, assuming a large-scale ammonia trade from Australia to Germany and including taxes on CO_2. Their study obtained costs of about 570, 500 and 650 €/tNH3 (110, 97 and 126 €/MWh) for green, blue and grey ammonia, respectively.

In the present work, an economic comparative assessment of various ammonia production pathways is conducted using the LCOA methodology. In particular, this study investigates both PEMEC and SOEC as representatives of low- and high-temperature water electrolysis technologies, respectively, with SMR included as a benchmark for comparison. The main components of the plants are modelled to accurately capture their electrical and thermal energy consumption. Additionally, a detailed evaluation of the polarisation curves for the two electrolysis

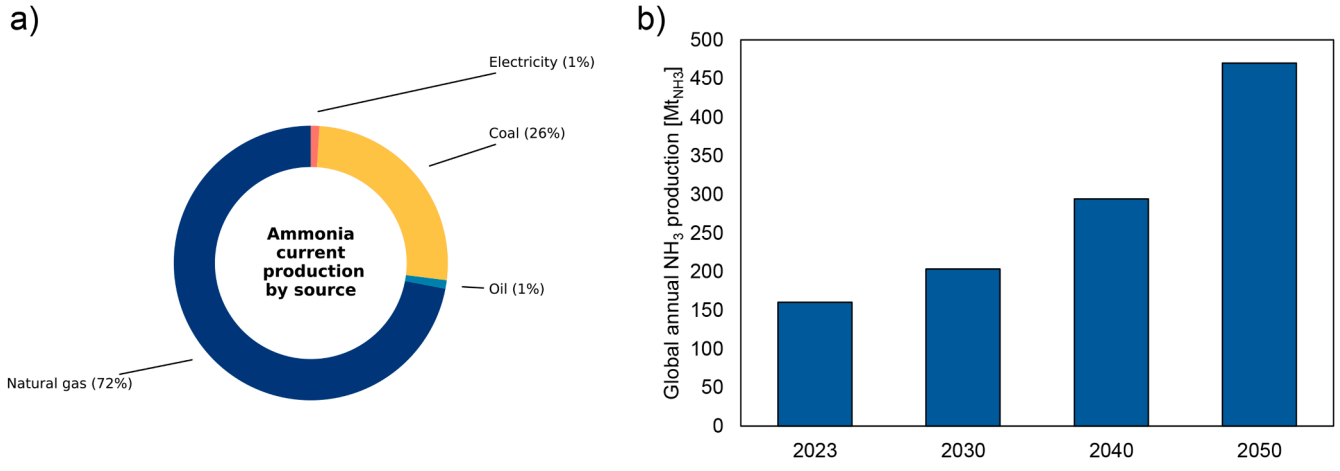

Fig. 1. (a) Current ammonia production by source [14]. (b) Expected global ammonia demand [7].

technologies is included, validated by fitting to experimental data from previous studies. To the best of our knowledge, no prior research has offered a detailed techno-economic evaluation of all three pathways, which is essential for a clear understanding of the cost-effectiveness of competing solutions. In addition, this study conducts extensive sensitivity analyses on electricity and gas prices under current and future market scenarios (2030 and 2040), identifying the specific conditions under which each pathway becomes preferable. Unlike previous studies, which only evaluated the impact of a carbon tax on electrolysis competitiveness over SMR in broad terms [31], this analysis is specifically tailored to the European market. It determines the carbon tax thresholds required in each European country, depending on its unique electricity and gas prices, to achieve cost parity between SMR and electrolyser technologies.

Moreover, many previous studies on SOEC technology did not explore the potential for recovering waste heat from the Haber-Bosch process for steam production. In contrast, this analysis includes a complete heat integration between the various components to assess the benefits of exploiting waste heat from the Haber-Bosch system.

Lastly, among the above-mentioned studies, only Mersch *et al.* [24] assessed the carbon footprint of electrolytic ammonia. Other studies either implicitly or explicitly assumed that the carbon intensity of the electricity used by the electrolyser is negligible, treating hydrogen from electrolysis as carbon-free. In contrast, this study provides a thorough assessment of CO_2 emissions associated not only with the SMR process (i.e., direct emissions) but also with the electrolysis-based pathways (i.e., indirect emissions from electricity). Additionally, fugitive methane emissions and CO_2 emissions linked to the extraction and transport of natural gas are considered for a comprehensive assessment of the ammonia carbon footprint. Furthermore, the analysis identifies the thresholds of electricity carbon intensity at which electrolysis-based ammonia production becomes more advantageous, in terms of CO_2 emissions, compared to the conventional SMR-based configuration.

The paper is structured as follows: Section 2 describes the complete methodology employed for the analysis, including a detailed modelling of the main components of the different plants. Results are presented and discussed in Section 3, and conclusions are drawn in Section 4.

2. Methodology

Sub-Section 2.1 provides an overview of the three plants along with a summary of their main techno-economic parameters. Detailed descriptions and modelling of the components are presented in sub-Sections 2.2 to 2.6. Sub-Section 2.7 outlines the forecasted parameters for analysing two future scenarios. Finally, a description of the LCOA approach is proposed in sub-Section 2.8, while the methodology for emissions assessment is detailed in sub-Section 2.9.

2.1. Plant designs

Three plant designs are included in the study, where the main difference stands in the hydrogen production system: (1) steam methane reformer, (2) proton exchange membrane electrolyser and (3) solid-oxide electrolyser. In parallel with the electrolyser or SMR, the Air Separation Unit (ASU) is needed for nitrogen production. Downstream of the nitrogen and hydrogen production, two compressors and two high-pressure tanks are modelled to ensure a constant flow of reagents at the correct pressure levels to the Haber-Bosch reactor. The HB reactor is integrated with the SOEC and SMR units, allowing waste heat from the ammonia synthesis reaction to be recovered in the hydrogen production process, thereby minimising energy consumption. In all configurations, the needed electrical power is assumed to be supplied by the grid, so no power production plant is modelled. All three plants are designed to guarantee an ammonia production rate of 10 tNH_3/h, chosen as representative of current operating plants [25,32]. Fig. 2 presents the schematic diagrams of the three configurations, while Table 1 summarises

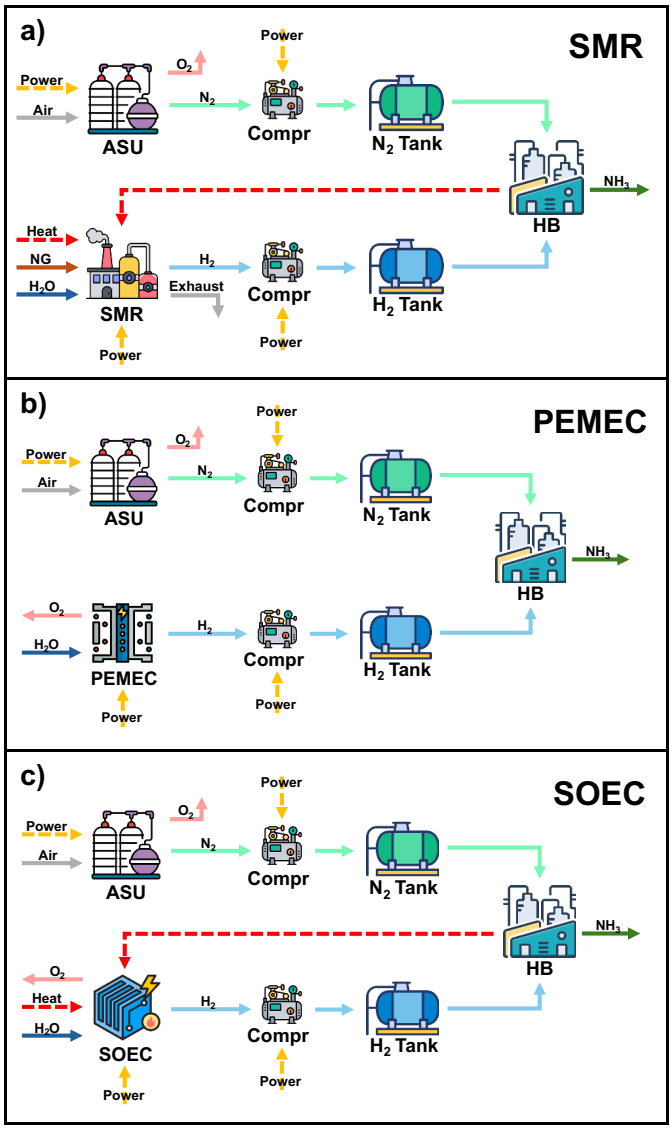

Fig. 2. Process layouts of ammonia production plants based on SMR (a), PEMEC (b) and SOEC (c). Main differences between the plants are represented by the hydrogen production systems and their heat integration with Haber-Bosch reactor.

Table 1
Main economic and technical parameters of the three ammonia productions plants. Prices of electricity, natural gas and CO_2 emissions are chosen as representative of European scenario in 2023.

	SMR	PEMEC	SOEC	Unit
Plant production	10	10	10	tNH_3/h
Plant lifetime	25	25	25	years
Interest rate	5	5	5	%
Annual operating hours	8712	8712	8712	h/y
Electricity price	0.10	0.10	0.10	€/kWh_e
NG price	0.05	–	–	€/kWh_{th}
CH_4 content in NG	95	–	–	% molar
CO_2 tax	80	–	–	€/tCO_2

the main parameters of the plants and the economic assumptions for the base scenario. Electricity and gas prices are based on average values from the European market, considering 2023 as the reference year [33,34]. Additionally, sensitivity analyses on these prices are included in the Results section. The cost associated with CO_2 emissions is assumed equal

to the cost of emissions allowances under the European Trading System (ETS) [35], considering average 2023 prices for the reference scenario [36]. For simplicity, this parameter will be referred to as the "CO_2 tax" throughout the rest of the document. While for calculation of CO_2 tax only direct emissions are accounted, both direct and indirect emissions are considered in this study for a complete evaluation of the carbon intensity of the three plants.

2.2. Steam methane reforming

Steam methane reforming remains the predominant hydrogen production method at global level, despite recent interest in electrochemical-based alternatives. The thermochemical conversion of methane is strongly endothermic, requiring high temperatures to occur efficiently (~800°C):

$$CH_4 + H_2O \rightarrow 3H_2 + CO \quad \Delta h = 206 \frac{kJ}{mol} \tag{1}$$

where Δh is the standard enthalpy of reaction (calculated at 298 K). To maximise the hydrogen production, the Water Gas Shift (WGS) reaction is operated downstream:

$$CO + H_2O \rightarrow H_2 + CO_2 \quad \Delta h = -41 \frac{kJ}{mol} \tag{2}$$

where the standard enthalpy of reaction indicates that the reaction is exothermic. The overall reaction of the system can be rewritten as:

$$CH_4 + 2H_2O \rightarrow 4H_2 + CO_2 \quad \Delta h = 165 \frac{kJ}{mol} \tag{3}$$

The WGS generally occurs at lower temperatures than the SMR [37], with reactors at different temperature levels (200–250°C and 350–450°C [37]), exploiting different types of catalysts. The use of different temperature levels allows for heat integration between the fluxes entering and exiting the reformer and the WGS reactors, to reduce the heat demand of the plant. Generally, a plant consists of an SMR reactor followed by two WGS reactors and one or more purification components, usually based on the Pressure Swing Adsorption (PSA) process [38]. The plant scheme is shown in Fig. 3.

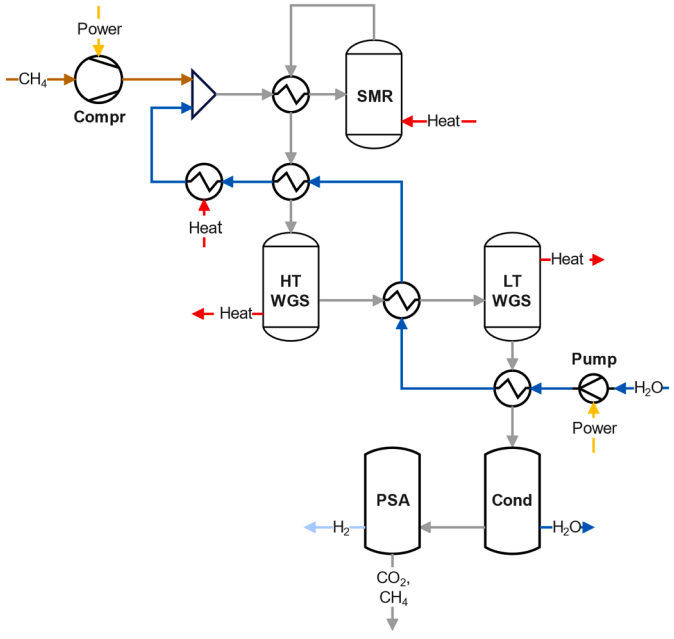

Fig. 3. SMR process layout. A SMR reactor is assumed, followed by two WGS reactors, a condenser for water removal and a purification unit based on PSA. A detailed stream table of the process model is available in the Supplementary Material.

The system is assumed to operate at three temperature levels, respectively equal to 800°C, 350°C and 200°C, and at a pressure of 24 bar. This pressure is chosen to ensure that the minimum pressure at the PSA remains above 20 bar, which is essential for its proper functioning [39]. The plant is mainly composed of a compressor and a pump (respectively operating on natural gas and water), pre-heaters, heat exchangers, one SMR reactor, two WGS reactors (HT WGS and LT WGS in Fig. 3), a condenser (Cond in Fig. 3) for the removal of the unreacted water and a PSA for H_2 purification. Heat integration is not only operated between the components of the SMR plant but is also analysed in order to connect the SMR and HB plants. As described in sub-Section 2.6, the HB reactors are strongly exothermic and provide heat at about 400°C. This thermal energy can be exploited by the SMR, considering that the two plants are assumed to operate mostly simultaneously. The additional heat that cannot be provided by the HB is assumed to be provided by gas burners. In Table 2, the operating parameters of the SMR system are summarised, along with its Specific Electricity Consumption (SEC) and Specific Heat Consumption (SHC). Electrical consumption is primarily attributed to the NG compressor and the water pump, while gas consumption is due to both the SMR reaction and the thermal needs of the plant, which are met using gas burners.

2.3. Electrolyser

Two main technologies are analysed as electrolysers: PEMEC and SOEC. To properly evaluate their energy consumptions, the electrochemical models of both types of electrolysers are studied. Specifically, their polarisation curves are modelled and subsequently calibrated with experimental data. For this purpose, various parameters of the electrochemical models are chosen as fitting variables. Model calibration is carried out by minimising the sum of the squared difference between model and experimental values of the cell operating voltage.

Once the polarisation curve is defined, the plant system can be designed with inclusion of the Balance Of Plant (BOP), in order to properly evaluate the working conditions of the entire system and in particular its SEC for both the PEMEC and SOEC cases.

2.3.1. PEMEC

First, the polarisation curve of the PEMEC is derived. Experimental data provided by Crespi *et al.* [41] are used to calibrate the model. A summary of the used methodology, equations and model parameters, including those assumed from literature and those derived through calibration, can be found in the Supplementary Material. Given the polarisation curve, which defines the cell voltage V_{cell} (V) as function of the current density i (A/m^2), the electrical power of the stack P (in W) is

Table 2
SMR specifics. For values where a reference is not provided, the specifics are determined based on the system modelling.

SMR	Specific	Unit	Reference
CAPEX	1800	€/(kg_{H2}/day)	[40]
M&R	4	% of CAPEX per year	[24]
Size	42,360	kg_{H2}/day	–
H_2 production	1765	kg_{H2}/h	–
Lifetime	25	years	[24]
Operating pressure	24	bar	[38]
Operating temperature (max level)	800	°C	[40]
NG in SMR*	3716	kg_{NG}/h	–
SEC	0.48	kWh_e/kg_{H2}	–
SHC heaters**	10.1	kWh_{th}/kg_{H2}	–

* Natural gas used directly in the SMR to produce H2 (so, burners consumption is not considered).

** Heaters specific consumption is here reported net of the integration with the HB system (the gross SHC for heaters, without integration, would be 11.2 kWh_{th}/kg_{H2}).

provided by:

$$P = n_c \cdot V_{cell} \cdot i \cdot A \quad (4)$$

where A is the cell area (in m^2) and n_c is the number of cells of the stack.

The heat generated by the stack operation Φ (in W) can also be computed according to Eq. (5):

$$\Phi = -A \cdot n_c \cdot i \cdot \left(\frac{\Delta h}{2 \cdot F} - V_{cell} \right) \quad (5)$$

where Δh (in J/mol) is the change of enthalpy in the reaction of water electrolysis. It should be noted that a negative value for Φ indicates that the stack operates in endothermic mode, while a positive value signifies exothermic operation.

Hydrogen produced by the stack n_{H2} (in mol/s) is calculated as:

$$n_{H2} = \frac{\eta_F \cdot n_c \cdot i \cdot A}{2 \cdot F} \quad (6)$$

where η_F is the Faraday efficiency, which is defined according to the equation reported by Yodwong *et al.* [42]:

$$\eta_F = a \cdot i^b + c \quad (7)$$

The values assumed for the parameters a, b and c are reported in Table S.2. (Supplementary Material).

The auxiliary components of the PEMEC plant are then considered in order to accurately estimate its BOP energy consumption. The overall layout of the PEMEC plant is shown in Fig. 4.

The assumed operating temperature and pressure of the stack are 60°C and 30 bar, respectively. This pressure level is achieved using a hydraulic pump that increases the water pressure before it enters the cell. The cell operates in exothermic mode, so the pre-heating needed by the inlet make-up water (to compensate for the water consumed by the electrolysis reaction) is provided by heat integration with the outgoing flows from the stack, which are recirculated back to the inlet. The operating conditions of the electrolyser are shown in Table 3. The stack itself accounts for over 93% of the total electricity consumption, while the remaining percentage is attributed to the hydraulic pumps. These results are generally consistent with previous literature studies [43].

2.3.2. SOEC

Semi-empirical parameters for the definition of the polarisation curve of the cell are derived based on fitting the experimental curve provided by Hauch *et al.* [47]. As reported by Hauch et al. [47], high-temperature cells achieve greater efficiency due to the lower power demand for the same hydrogen output. The methodology, equations and

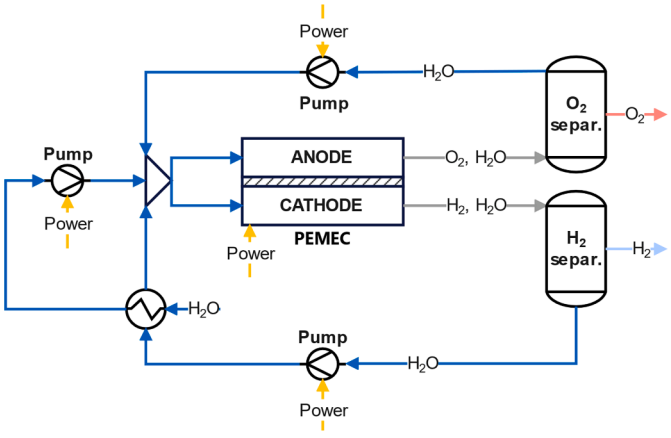

Fig. 4. PEMEC process layout. The stack is assumed to operate at 60°C and 30 bar. A detailed stream table of the process model is available in the Supplementary Material.

Table 3
PEMEC specifics. For values where a reference is not provided, the specifics are determined based on the system modelling. Supplementary material provides a sensitivity analysis on the results (in terms of both costs and emissions), including different PEMEC technologies and their likely efficiency ranges.

PEM	Specific	Unit	Reference
CAPEX	1200	€/kW	[44]
M&R	4	% of CAPEX per year	[31]
Size	94.7	MW_e	–
H_2 production	1765	kg_{H2}/h	–
Stack lifetime	10	years	[31]
BOP lifetime	25	years	[31]
Replacement cost	27	% of CAPEX	[45]
Operating pressure	30	bar	[41]
Operating temperature	60	°C	[46]
Operating voltage	2.04	V	–
Operating current density	2	A/cm^2	–
SEC stack	55.7	kWh_e/kg_{H2}	–
SEC BOP	4.0	kWh_e/kg_{H2}	–

model parameters, including those assumed from literature and those derived through model calibration, can be found in the Supplementary Material. Once the polarisation curve is defined, Eqs. (4)–(6) are also applicable to the SOEC for estimating the electrical and thermal power of the stack, as well as the produced hydrogen. The Faraday efficiency η_F is assumed to be 0.98 [48].

The SOEC, assumed to operate at 800°C, is then modelled with its BOP, including a heat integration between streams entering and exiting the stack, in order to minimise the thermal requirements for water pre-heating. Plant design is developed starting from the work by Zhao *et al.* [49], and a scheme is reported in Fig. 5.

Considering a proper heat integration, the thermal need for water pre-heating can be divided into two temperature levels: approximately 110°C and 800°C. Heaters are necessary to pre-heat the flows entering the SOEC stack, as heat integration with the flows exiting the SOEC stack is insufficient. The 800°C thermal need must be necessarily provided by an external source (here, an electric heater is assumed), as the system does not include any other heat source at this temperature. Instead, the thermal need at 110°C can be partially fulfilled by the HB reactors. Since the SOEC is generally assumed to operate simultaneously with the HB system, part of the SOEC thermal needs can be satisfied through a thermal integration with the HB system. This integration reduces overall energy requirements and results in notable economic savings. However, because the heat from the HB is not sufficient, the remaining thermal energy is provided through the use of electric heaters, operating at 110°C and 800°C.

Table 4 presents the main economic parameters and operating conditions, including the hydrogen production and power consumption of the various system components. It is evident that the stack is the major power consumer, accounting for about 86% of the total consumption of the electrolyser system. The second-largest energy consumers are the electric heaters, which operate at 110°C and 800°C, contributing around 13% of the overall electrical consumption. Lastly, approximately 1% of the power consumption is due to the pump and the compressors. These results align with other studies that incorporate heat integration in high-temperature electrolyser systems [50]. It should be noted that the SOEC is assumed to operate under thermoneutral conditions, so the stack itself does not need an external heat source.

2.4. Air separation unit

Given the large scale of the plant, cryogenic distillation is selected as the most effective technology for the air separation unit (necessary for nitrogen production) [53]. To achieve the high purity of nitrogen required by the HB reactor and prevent O_2 and H_2O from damaging the catalysts [54], a multi-column ASU is necessary. In particular, in the considered plant, a two-column ASU is used, consisting of a High

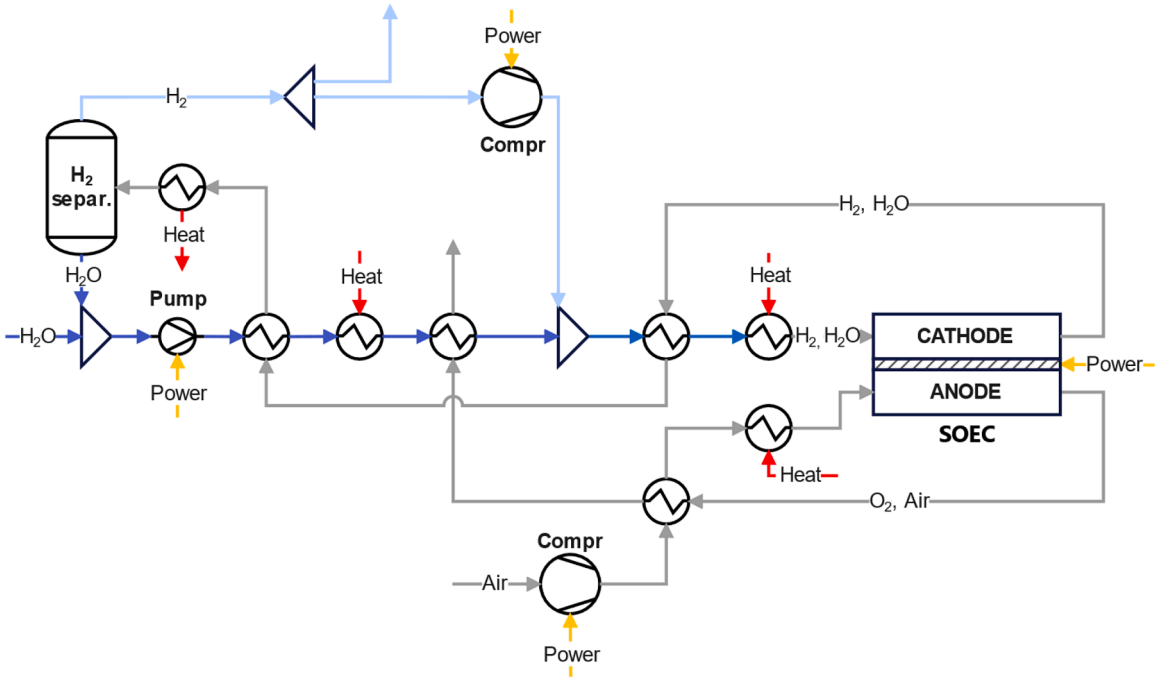

Fig. 5. SOEC process layout. The stack is assumed to operate at 800°C and 1.1 bar. Part of the heat needed by the electrolyser is assumed to be provided by the HB system. A detailed stream table of the process model is available in the Supplementary Material.

Table 4
SOEC specifics. For values where a reference is not provided, the specifics are determined based on the system modelling. Supplementary material provides a sensitivity analysis on the results (in terms of both costs and emissions), including different SOEC technologies and their likely efficiency ranges.

SOEC stack and BOP	Specific	Unit	Reference
CAPEX	2250	€/kW	[51]
M&R	4	% of CAPEX per year	[52]
Size	62.4	MW_e	–
H_2 production	1765	kg_{H2}/h	–
Stack lifetime	6	years	[25]
BOP lifetime	25	years	[25]
Replacement cost	23	% of CAPEX	[52]
Operating pressure	1.1	bar	[52]
Operating temperature	800	°C	[47]
Operating voltage	1.29	V	–
Operating current density	1.8	A/cm^2	–
SEC stack	35.4	kWh_e/kg_{H2}	–
SEC BOP (excluding heaters)	0.3	kWh_e/kg_{H2}	–
SEC heaters	5.5*	kWh_e/kg_{H2}	–

* Heaters specific consumption is here reported net of the integration with the HB system (the gross SEC for heaters, without integration, would be 7.8 kWh/kg_{H2}).

Pressure Column (HPC) and a Low Pressure Column (LPC). The main components of the system include: compressors (generally multistage with intercooling, which account for the largest portion of power consumption), air purificators (usually pressure or thermal swing adsorption), heat exchangers, and cryogenic distillation columns (one operating at about 5.2 bar and the other at 1.4 bar [55]), which are thermally coupled. The plant layout is shown in Fig. 6, based on designs by Cheng et al. [55] and Agrawal *et al.* [56].

Plant parameters, including the specific consumption of the ASU, are detailed in Table 5. The energy needs of the system are consistent with findings from other studies [57].

2.5. Compressors and storages

Compressed hydrogen and nitrogen storage systems are included in the ammonia production plant. Although the plant is assumed to operate continuously (meaning the storage tanks would not be strictly necessary for most of the year), small storage buffers for both hydrogen and nitrogen are considered useful. This is because the HB system is negatively affected by shutdowns, and these buffers help reduce the frequency of interruptions in its operation.

Since the Haber-Bosch process operates at about 300 bar, both hydrogen and nitrogen are stored in buffer tanks in gaseous form at 350 bar This solution is justified considering that a compression stage would be necessary to meet the requirements of the HB process. Other storage solutions, such as liquid hydrogen or higher-pressure gaseous storage, are not considered as these plants typically do not face space limitations. For both hydrogen and nitrogen, three stages of compression are assumed, followed by a tank.

The capacities of the tanks are designed to ensure 48 h of autonomy, allowing for potential maintenance periods for the hydrogen production systems or the ASU. Table 6 presents the main parameters of the two compressors and the two tanks.

2.6. Haber-bosch reactor

The Haber-Bosch process is still the most widely adopted process for ammonia production. The ammonia production reaction is here reported:

$$N_2 + 3H_2 \leftrightarrow 2NH_3 \;\; \Delta h = -92\frac{kJ}{mol} \tag{8}$$

where Δh is the standard enthalpy of reaction (calculated at 298 K). To increase the production rate, the reactor generally operates at high pressure (250–300 bar). Although low temperatures would favour the reaction due to its exothermic nature, the temperature must be maintained at around 400°C to enhance reaction kinetics and effectively

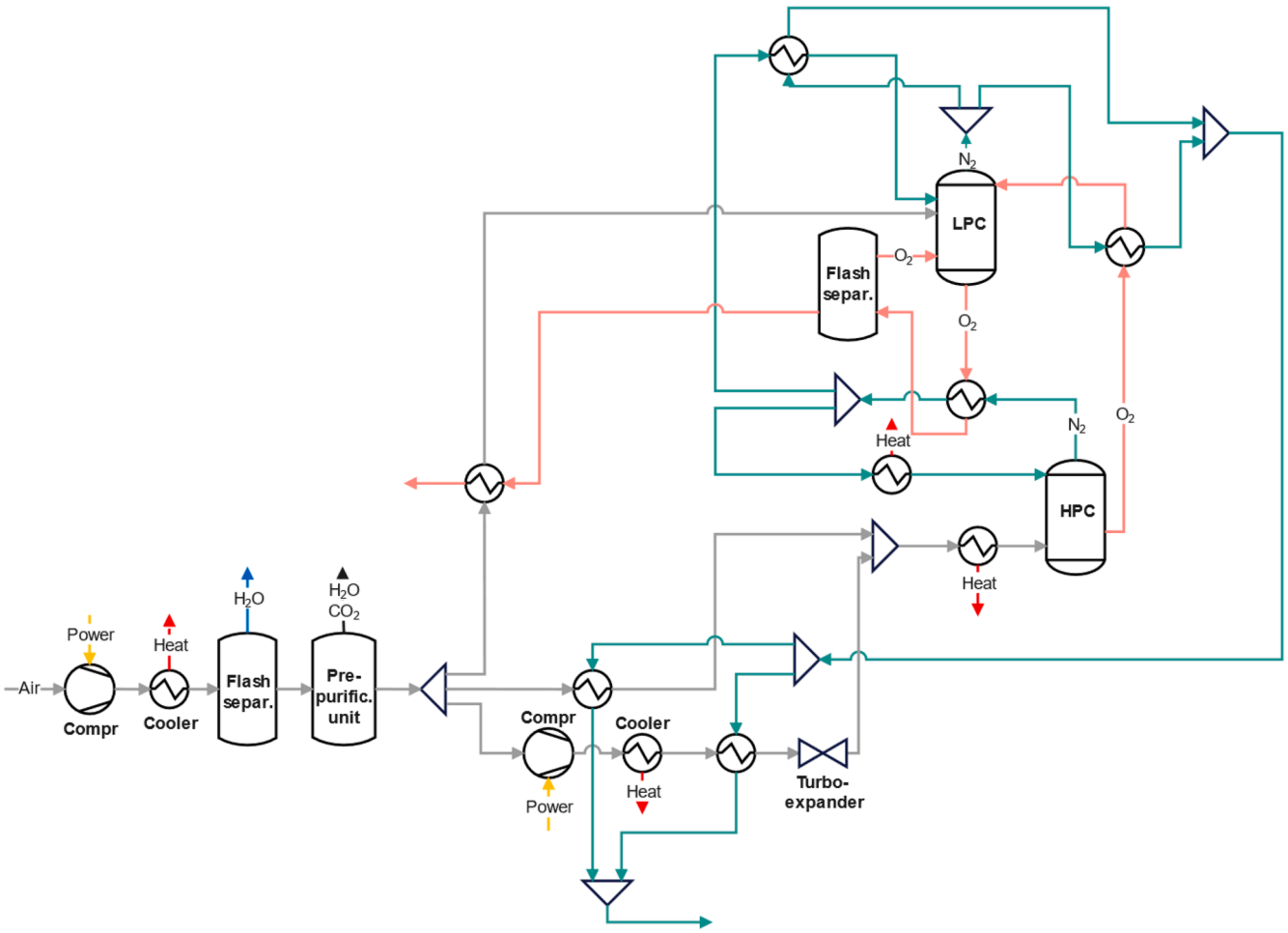

Fig. 6. ASU process layout, based on two-column cryogenic distillation plant. A detailed stream table of the process model is available in the Supplementary Material.

Table 5
ASU specifics. For values where a reference is not provided, the specifics are determined based on the system modelling.

ASU	Specific	Unit	Reference
CAPEX	1450	€/(kg_{N2}/h)	[32]
M&R	2	% of CAPEX per year	[32]
Size	8235	kg_{N2}/h	–
Lifetime	25	years	[23]
SEC	0.095	kWh_e/kg_{N2}	–

utilise the iron catalyst [54]. To prevent excessive temperature increases and to improve the conversion rate, multiple reactors are usually employed. The temperature at the entrance of each reactor is set to 400°C, but it increases during the process due to the exothermicity of the reaction. At the outlet of each reactor, the temperature is brought back to 400°C, thanks to thermal integration with internal streams (e.g. pre-heating of inlet gases) for reactors 1 and 3 and with the electrolysers or the SMR sections (reactor 2). The plant is assumed to have three reactors, but even with this configuration, the outlet stream remains rich in unreacted nitrogen and hydrogen. For this reason, a strong recirculation is necessary, including a compression stage to compensate for pressure losses along the plant. Specifically, the recirculated stream accounts for 58% (by mass) of the total inlet gas at the mixer feeding the HB reactors. The layout of the HB process is illustrated in Fig. 7.

The synthesis loops are designed to operate under steady-state conditions most of the time, as shutdowns or excessively fast ramp-ups could damage the reactors, particularly the iron catalysts. Table 7 presents the main parameters and energy consumption for the HB system. Since hydrogen and nitrogen compression occurs upstream of the two tanks, the power consumption of the HB is very low, as it is only required for compressing the recirculating stream to compensate for pressure losses.

2.7. Future scenarios

An additional analysis is conducted to evaluate the technical and economic developments of the considered technologies and to identify potential trends for future ammonia production. This assessment includes projections for the years 2030 and 2040, focusing on PEMEC and SOEC technologies. In contrast, the SMR system, given its maturity and established market presence, is assumed to maintain constant performance and cost metrics.

Specifically, PEMEC and SOEC are projected to show improvements in stack energy consumption and cost reductions. All other plant components, including the HB system, ASU, compressors and storage tanks, are assumed to retain their current economic and performance parameters. Table 8 summarises the assumed parameters for the future scenarios assessment, based on estimates provided by Böhm *et al.* [51].

Table 6
Compressors and storage tanks for hydrogen and nitrogen. For values where a reference is not reported, the specifics are determined based on the system modelling.

H_2 compressor	Specific	Unit	Reference
CAPEX	11,000	€/(kg_{H2}/h)	[32]
M&R	1	% of CAPEX per year	[58]
Lifetime	25	years	[32]
Size	1765	kg_{H2}/h	–
p_{in} (SMR/PEMEC/SOEC)	20/29/1	bar	–
p_{out}	350	bar	–
SEC (SMR/PEMEC/SOEC)	1.78/1.52/3.81	kWh_e/kg_{H2}	–
H_2 tank	**Specific**	**Unit**	**Reference**
CAPEX	470	€/kg_{H2}	[32]
M&R	1	% of CAPEX per year	[58]
Lifetime	25	years	[32]
Pressure	350	bar	–
Size	84,700	kg_{H2}	–
N_2 compressor	**Specific**	**Unit**	**Reference**
CAPEX	2200	€/(kg_{N2}/h)	[54]
M&R	1	% of CAPEX per year	[58]
Lifetime	25	years	[59]
Size	8235	kg_{N2}/h	–
p_{in}	1	bar	–
p_{out}	350	bar	–
SEC	0.27	kWh_e/kg_{N2}	–
N_2 tank	**Specific**	**Unit**	**Reference**
CAPEX	31	€/kg_{N2}	[60]
M&R	1	% of CAPEX per year	[58]
Lifetime	25	years	[60]
Pressure	350	bar	–
Size	395,300	kg_{N2}	–

2.8. Levelised cost of ammonia

The three ammonia production plants (i.e., based on PEMEC, SOEC and SMR) are compared from an economic perspective, under both current and future scenarios, to assess the cost-competitiveness of each solution depending on the background conditions. The Levelised Cost Of Ammonia (LCOA) is chosen to present a direct economic comparison between the different production processes. It includes all the costs associated with the production of ammonia into a single indicator, encompassing both capital and operational expenditures over the plant's lifetime. The LCOA (in €/tNH_3) is calculated according to the following expression:

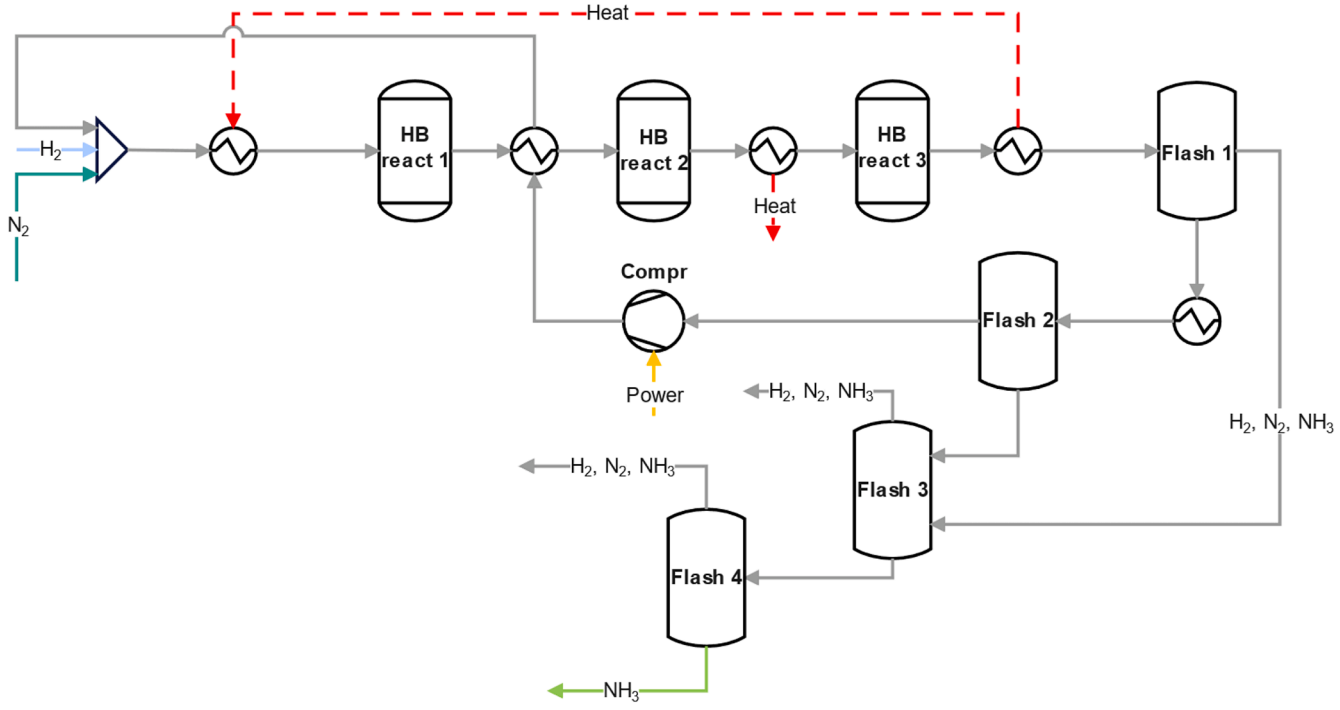

Fig. 7. HB process layout, composed of three reactors and four separation stages. A detailed stream table of the process model is available in the Supplementary Material.

Table 7
HB specifics. For values where Reference is not reported, the specifics were determined basing on the modelling of the system.

HB	Specific	Unit	Reference
CAPEX	3000	€/(kg_{NH3}/h)	[32]
M&R	2	% of CAPEX per year	[61]
Size	10,000	kg_{NH3}/h	–
Lifetime	25	years	[23]
SEC	0.002	kWh_e/kg_{NH3}	–

$$LCOA = \frac{\sum_{i=1}^{N} \frac{I_i+O_i}{(1+d)^i}}{\sum_{i=1}^{N} \frac{M_{NH3,i}}{(1+d)^i}} \tag{9}$$

where I_i and O_i (in €) represent the investment and operational expenditures for the i-th year, respectively, $M_{NH3,i}$ (in t) is the ammonia produced in the i-th year, d (in %) is the annual discount rate and N is the final year of the analysis. The investment cost I_i includes all CAPEX parameters outlined in previous sections, depending on the specific costs and the sizes of the components. The operational cost O_i is evaluated as the sum of maintenance (M&R, including stack replacement for the electrolysers), energy costs (covering electricity and gas costs) and carbon taxes (for the SMR case).

2.9. Specific CO_2 emissions

This study also focuses on the operational CO_2 emissions of the three investigated plant layouts. CO_2 emissions during operation consist of two contributes: direct and indirect emissions. Direct emissions arise from the combustion/conversion of fossil fuels and are the only emissions subject to CO_2 tax. The electrolysis-based layouts (SOEC and PEMEC) do not require fossil fuels as input and therefore do not produce direct CO_2 emissions. In contrast, in the SMR plant, CO_2 is emitted during H_2 production and thermal energy generation using natural gas burners. Direct Specific Emissions (SE_d) (in tCO_2/tNH_3) are calculated according to Eq. (10):

$$SE_d = \frac{\sum_{i=1}^{N} M_{CH4,i} \cdot \varepsilon_{CH4,d}}{\sum_{i=1}^{N} M_{NH3,i}} \tag{10}$$

where $M_{CH4,i}$ (in t) is the methane used in the i-th year (for both hydrogen production and thermal energy) and $\varepsilon_{CH4,d}$ (in tCO_2/tCH_4) is the specific methane emissions, indicating the mass of CO_2 emitted per unit mass of CH_4 used (equal to 2.75 tCO_2/tCH_4). A detailed description of $\varepsilon_{CH4,d}$ is provided in Supplementary Material).

Indirect emissions encompass those associated with electricity use and emissions from natural gas extraction and transport, including equivalent CO_2 emissions due to methane leakages during the transport phase. These emissions are needed for providing a comprehensive assessment of the ammonia carbon footprint across the three production pathways, not limited to direct emissions. Indirect Specific Emissions (SE_{id}) (in tCO_2/tNH_3) are calculated as follows:

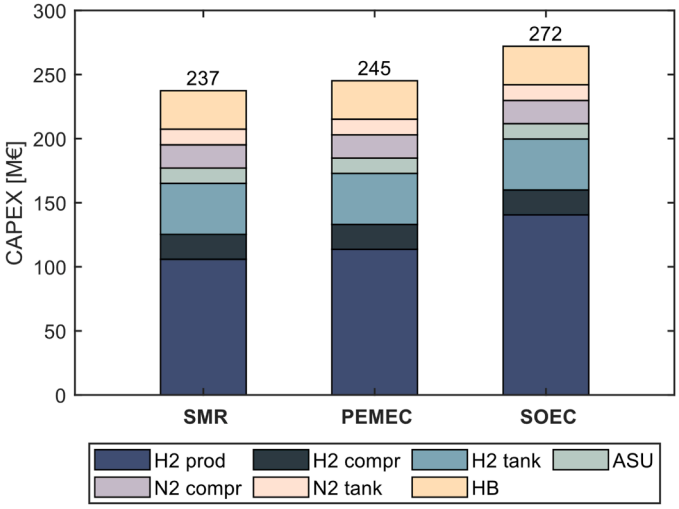

Fig. 8. Capital expenditure (CAPEX) of the three plants. Category indicated as "H2 prod" indicates the hydrogen production system associated to the plant (in order, SMR, PEMEC and SOEC), and it represents the main cost-impacting component. Additional details on the CAPEX breakdown are provided in the Supplementary Material.

$$SE_{id} = \frac{\sum_{i=1}^{N} \left(E_{el,i} \cdot \frac{\varepsilon_{grid}}{10^6} \right)}{\sum_{i=1}^{N} M_{NH3,i}} + \frac{\sum_{i=1}^{N} \left(M_{CH4,i} \cdot \frac{\Delta h_{CH4} \cdot \varepsilon_{CH4,up}}{10^3} \right)}{\sum_{i=1}^{N} M_{NH3,i}} + \frac{\sum_{i=1}^{N} \left(M_{CH4,i} \cdot \lambda_{CH4} \cdot GWP_{CH4} \right)}{\sum_{i=1}^{N} M_{NH3,i}} \tag{11}$$

where $E_{el,i}$ (in kWh_e) is the electrical energy used by the plant in the i-th year, ε_{grid} (in gCO_2/kWh_e) is the carbon intensity of the used electricity, Δh_{CH4} (kWh_{th}/kg) is the lower heating value of methane (equal to 13.90 kWh_{th}/kg), $\varepsilon_{CH4,up}$ is the upstream emission factor for CO_2 emissions associated with the production and transport of natural gas (assumed equal to 32 gCO_2/kWh_{th} [62]), λ_{CH4} is the fugitive emissions rate (assumed equal to 0.02 [63]) and GWP_{CH4} is the global warming potential of methane (assumed equal to 28 gCO_2/gCH_4 [64]).

The total Specific Emissions (SE) (in tCO_2/tNH_3) are obtained by summing the direct and indirect contributions:

$$SE = SE_d + SE_{id} \tag{12}$$

While only direct emissions are considered for calculating the carbon tax, this study includes both direct and indirect emissions for a complete evaluation of the carbon intensity of the three plants.

Table 8
Electrolyser parameters for future scenario assessment. Percentage reductions in CAPEX and SEC compared to current values are shown in parentheses. Strong CAPEX reductions are expected in the coming years, while SEC variations are less pronounced.

PEMEC	Current	2030	2040	Unit	Reference
CAPEX	1200	700 (−42%)	390 (−68%)	€/kW	[51]
SEC stack	55.7	50.9 (−5.2%)	49.1 (−8.5%)	kWh_e/kg_{H2}	[51]
SOEC	**Current**	**2030**	**2040**	**Unit**	**Reference**
CAPEX	2250	1270 (−44%)	670 (−71%)	€/kW	[51]
SEC stack	35.4	34.6 (−2.0%)	34.4 (−2.8%)	kWh_e/kg_{H2}	[51]

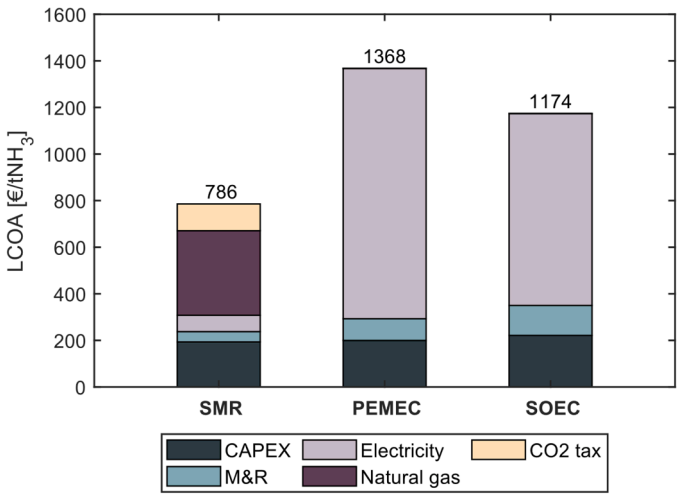

Fig. 9. LCOA for the investigated case study. "CAPEX" stands for Capital Expenditure of the three different plants. "CO2 tax" refers to carbon tax associated with emissions connected to natural gas use (assumed 80 €/tCO_2). In "M&R" (Maintenance and Repair costs) category, electrolysers replacement is included. Additional details on the LCOA breakdown are provided in Supplementary Material.

3. Results

This section presents and discusses the LCOA values for the different plants (sub-Section 3.2), with a detailed breakdown of their CAPEX to highlight the most impactful components (sub-Section 3.1). Following this, a sensitivity analysis on the prices of both natural gas and electricity is provided to offer a broader perspective on the viability of the various solutions (sub-Section 3.3). Sub-Section 3.4 includes forecasts and future scenarios from an economic standpoint, providing an overview of the competitiveness of the three technologies in the coming years. Finally, sub-Section 3.5 explores the CO_2 emissions associated with plant operation depending on the electricity carbon intensity.

3.1. Investment cost

The capital costs of the three ammonia production plants are presented in Fig. 8. The SMR- and PEMEC-based plants have comparable CAPEX (237 and 245 M€, respectively), while the SOEC-based plant is the most expensive configuration (272 M€).

The main cost-impacting component is the hydrogen production system, which varies depending on the configuration (i.e. SMR, PEMEC, and SOEC). The capital costs for SMR and PEMEC systems are relatively close, at 106 M€ and 114 M€, respectively. In contrast, the SOEC plant has a higher capital cost of 140 M€, reflecting its lower maturity and market penetration. Moving downstream in the hydrogen production chain, the H_2 compressor and storage tank also contribute significantly to the total cost (19 M€ and 40 M€, respectively). On the nitrogen side, components such as the air separation unit (ASU), N_2 compressor, and N_2 tank are less costly, despite the higher production rate of nitrogen compared to hydrogen (in terms of kg/h). This is due to the widespread use of these components in the market and the relatively simpler handling and storage of nitrogen compared to hydrogen. Finally, the HB system adds 30 M€ to the total CAPEX. Although this cost is non-negligible, it is worth noting that it is significantly lower than the cost associated with the hydrogen production.

3.2. Levelised cost of ammonia

Fig. 9 shows the resulting LCOA values for the different ammonia production methods (using reference electricity and NG prices of 0.10 and 0.05 €/kWh, respectively, as reported in Table 1). SMR emerges as the most cost-effective solution, with an ammonia production cost of approximately 786 €/tNH_3. Previous studies have generally reported lower costs for conventional ammonia production: for example, Zhang *et al.* [25] found costs below 400 USD/tNH_3, while Mersch et al. [24] reported values in the range 300–500 USD/tNH_3, depending on gas prices. However, the higher LCOA reported here can be attributed to two main factors. First, the assumed natural gas price of 0.05 €/kWh is based on European market prices [65], which are generally higher than those in many non-European countries (e.g., the USA [66]). Given that gas costs account for over 45% of the LCOA for SMR, a reduction in gas prices could significantly impact the total production costs (the impact of natural gas prices will be addressed in detail in sub-Section 3.3). Second, most previous analyses did not consider the costs associated with CO_2 emission taxes. Using a reference tax of 80 €/tCO_2 [36], this factor contributes approximately 115 €/tNH_3 (15%) to the LCOA.

Among the electrolytic hydrogen options, SOEC is the most cost-effective despite its higher capital costs and shorter lifetime compared to PEMEC, with LCOA values of 1174 €/tNH_3 for SOEC and 1368 €/tNH_3 for PEMEC. The cost-effectiveness of SOEC is attributed to its lower specific energy consumption (41.2 kWh_e/kg_{H2} for SOEC and 59.7 kWh_e/kg_{H2} or PEMEC), leading to lower electricity costs.

To thoroughly assess the cost-competitiveness between SMR and electrolyser-based solutions in European countries, a detailed analysis has been conducted, focusing on the impact of electricity and NG prices, as well as carbon taxes specifically targeting direct CO_2 emissions associated with NG use. The electricity and NG prices used in this analysis are tailored to each country and are based on data from the

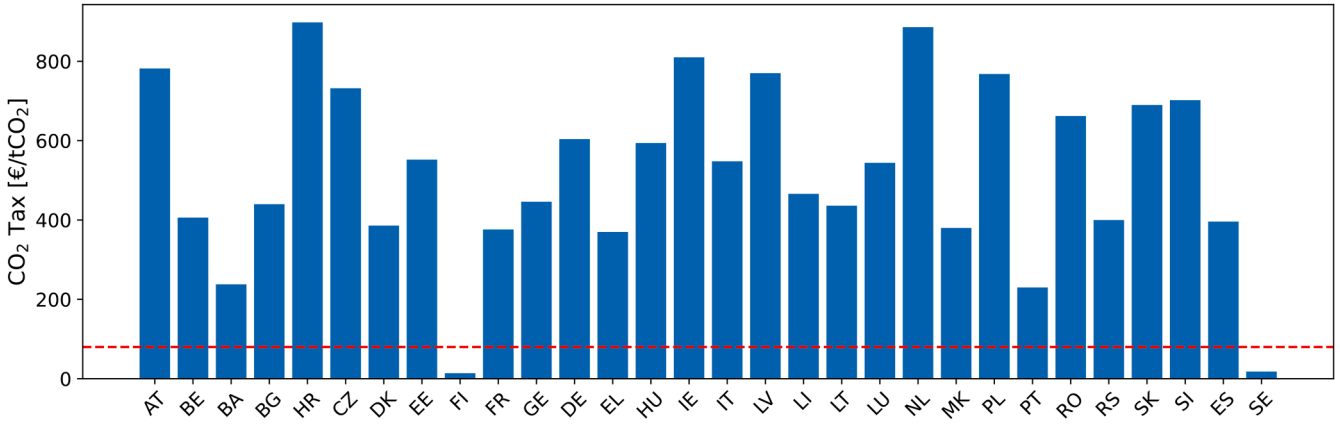

Fig. 10. CO2 tax required to achieve equal LCOA between SMR and the most cost-effective electrolyser solution in each European country. The red dashed line indicates 80 €/tCO_2, which is representative of the 2023 average value. Detailed data used for this figure are provided in the Supplementary Material.

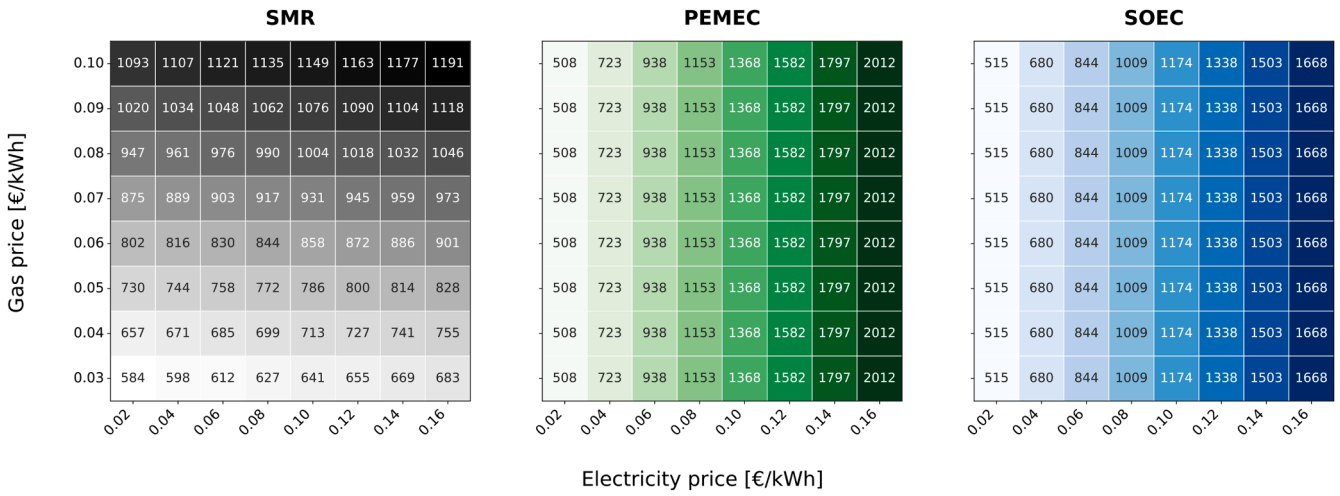

Fig. 11. LCOA (€/tNH$_3$) of the three technologies (SMR, PEMEC and SOEC) for different electricity and natural gas prices.

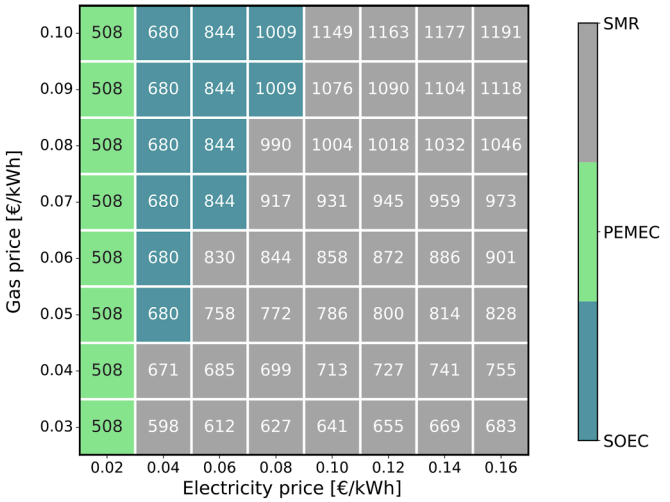

Fig. 12. Optimal LCOA [€/tNH$_3$] based on electricity and gas prices. The colour of each cell indicates the most cost-effective technology for a given combination of electricity and gas prices, while the number within the cell represents the corresponding LCOA. Electrolysers are competitive for electricity prices up to 0.08 €/kWh. Above this threshold, SMR is the most cost-effective solution for gas prices below 0.10 €/kWh.

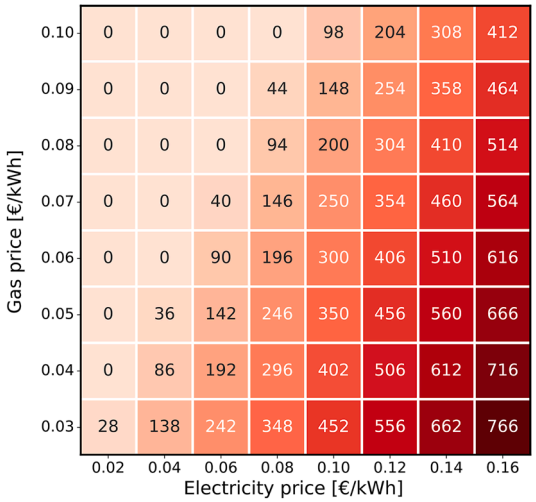

Fig. 13. Needed carbon tax (€/tCO$_2$) to achieve equal LCOA between SMR and the most cost-effective electrolyser solution with various electricity and natural gas prices.

second semester of 2023 as reported in the Eurostat database [33,34] (price values are provided in the Supplementary Material). Fig. 10 illustrates the required carbon tax in each country to achieve equal LCOA between SMR-based ammonia production and the most economically advantageous electrolyser plant. In countries such as Finland and Sweden, where electricity prices are notably low, cost parity can already be achieved with existing levels of carbon taxes. However, in many other countries, particularly those where NG prices are substantially lower than electricity prices (i.e., Netherland, Ireland, Croatia, Austria, etc.), achieving cost parity remains a significant challenge requiring relevant carbon penalties (up to approximatively 900 €/tCO$_2$). Overall, the analysis underscores that the carbon tax plays a crucial role in determining cost parity between SMR and electrolyser technologies and it could represent a possible alternative to a strict prohibition on the use of fossil hydrogen.

3.3. Impact of electricity and natural gas prices

Given the significant influence of both electricity and natural gas on the LCOA for the three plants, a sensitivity analysis on these two parameters is conducted. The price of electricity is explored within the range of 0.02–0.16 €/kWh, while the price of natural gas is assumed to vary between 0.03–0.10 €/kWh.

Fig. 11 presents the LCOA of the three technologies through three heatmaps, each corresponding to one technology. The values within each cell represent the LCOA for each combination of electricity and gas prices. The SOEC and PEMEC are affected solely by electricity prices, as both the electrolysers and heaters are powered by electricity. In contrast, SMR is influenced by both electricity and gas prices, with a more pronounced impact from gas prices.

Based on results from Fig. 11, Fig. 12 illustrates the most economical technology and its LCOA for each combination of electricity and gas prices. When electricity prices are very low (approximately 0.02 €/kWh$_e$, quite far from the current grid electricity prices, which reach a minimum of about 0.06 €/kWh$_e$ in Sweden and Portugal [33]), the PEMEC system is the most cost-effective option, as its high specific energy consumption does not reflect in high operation costs. In the

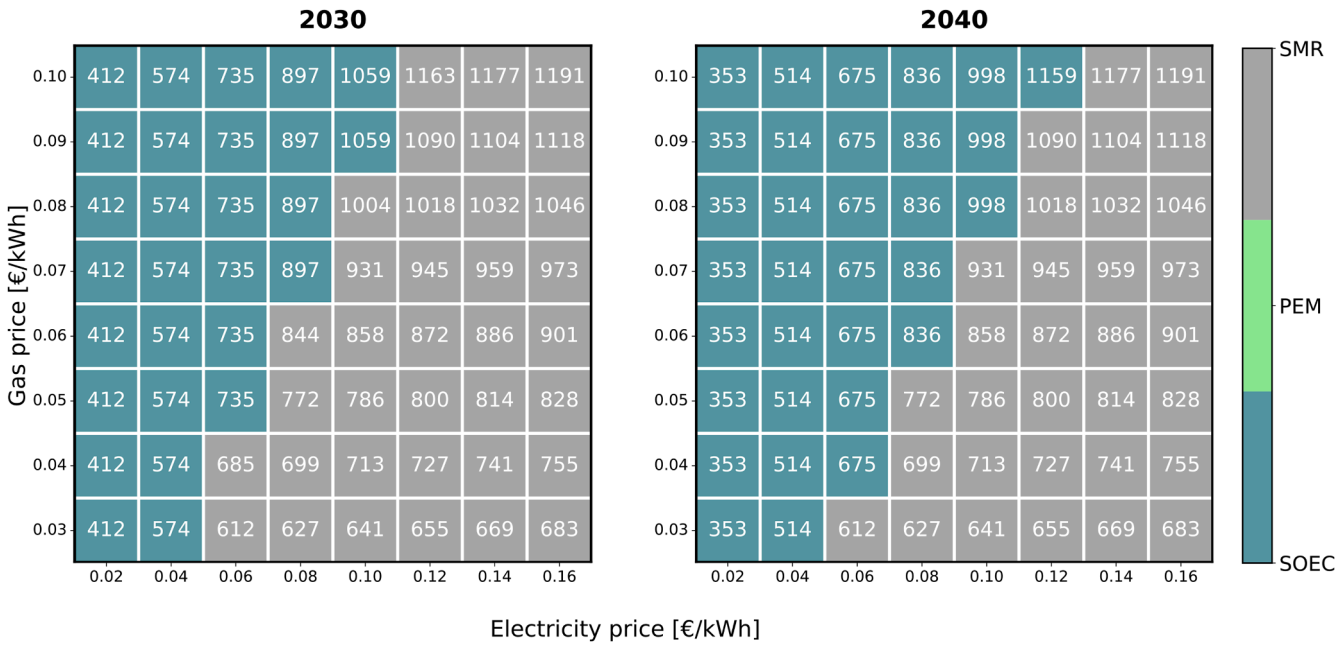

Fig. 14. Optimal LCOA [€/tNH3] based on electricity and gas prices in future scenarios (2030 and 2040). The colour of each cell indicates the most cost-effective technology for a given combination of electricity and gas prices, while the number within the cell represents the corresponding LCOA.

electricity price range of approximately 0.04 to 0.08 €/kWh$_e$, the optimal solution can vary: SMR represents the most cost-effective technology at low gas prices, while SOEC becomes the preferred option when gas prices are higher. For electricity prices of 0.10 €/kWh$_e$ or above, SMR emerges as the most cost-effective choice, even with high natural gas prices.

Fig. 13 shows the carbon tax needed to achieve equal LCOA between the SMR-based plant and the most cost-effective electrolysis solution. Locations with low electricity prices (on the left side of the heatmap) require low carbon taxes to incentivise carbon reduction. However, as shown in Fig. 10, very few European countries fall into this category. Conversely, regions with higher electricity costs (on the right side) necessitate significantly higher carbon taxes. This analysis suggests that differentiated carbon policies based on local energy prices (both within Europe and beyond) could be helpful to meet emission reduction goals.

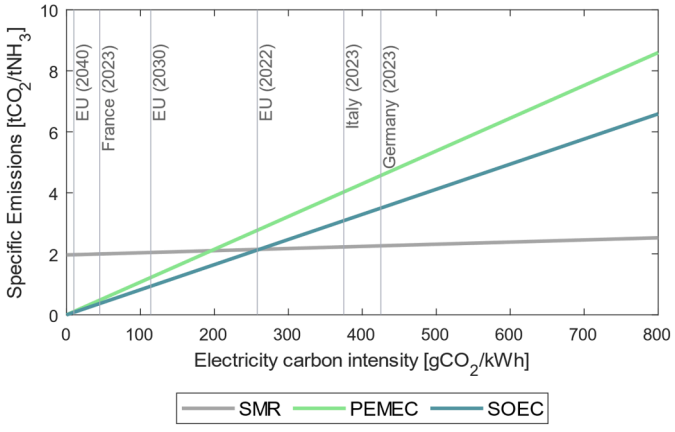

Fig. 15. Emissions associated to ammonia production varying the carbon intensity of the used electricity. Emissions parity between electrolysers and SMR is reached at 200 and 260 gCO2/kWh for PEMEC and SOEC respectively. Reference values referred to present are taken from Electricity Map [67], while future values are assumed from European Environment Agency [68] and European Commission forecasts [69].

3.4. Future scenario cost-competitiveness of the technologies

This section investigates the cost-competitiveness of the three plant layouts in future scenarios for the years 2030 and 2040. Technical and economic advancements are projected for SOEC and PEMEC technologies due to component development and market expansion, as detailed in Table 8. In these scenarios, illustrated in Fig. 14, SOEC emerges as the cost-optimal solution for various combinations of electricity and gas prices, particularly when electricity prices are below 0.08–0.10 €/kWh$_e$. Between 2030 and 2040, SOEC's presence in the heatmap increases due to a reduction in CAPEX, though the overall differences between the two scenarios are minimal. In both scenarios, PEMEC is not competitive with SOEC, as its lower CAPEX does not compensate for its higher specific electricity consumption. As a result, the primary alternatives are SOEC and SMR, with their competitiveness depending on electricity and gas prices. It is important to note that these scenarios assume a constant CO_2 tax of 80 €/tCO_2, since the high uncertainty associated with the European Emissions Trading System (ETS) [35] makes future price forecasts challenging. However, it is likely that this tax will increase in the coming years due to more stringent emission limits imposed by the European Union. An increase in the CO_2 tax would further enhance the economic feasibility of SOEC, even at higher electricity prices.

3.5. Specific CO_2 emissions

Traditional ammonia synthesis, which relies on fossil-derived hydrogen produced through SMR, significantly contributes to global carbon dioxide emissions. Utilising electrolytic hydrogen offers a promising pathway to decarbonise ammonia production and reduce dependency on finite resources. However, the carbon footprint of ammonia produced using electrolytic hydrogen deserves careful investigation. By analysing electricity consumption, fossil CO_2 emissions from combustion/conversion and the upstream emissions associated with fossil fuels, it is possible to determine the carbon intensity of the three investigated plant configurations, as outlines in Eqs. (10) and (11). This study helps identify the electricity carbon intensity thresholds required for electrolyser-based ammonia production to achieve lower emissions than the SMR-based alternative. Fig. 15 shows the specific CO_2 emissions (sum of direct and indirect contributions) associated with

ammonia production for the three hydrogen production technologies as a function of the carbon intensity of the used electricity. The carbon footprint of ammonia using water electrolysis is highly dependent on the carbon intensity of the electricity used to power the electrolyser. In contrast, emissions from SMR are relatively stable and only slightly increase with the carbon intensity of electricity, due to the low electricity consumption of the plant (associated with compressors, pumps, etc.). Moreover, PEMEC exhibits higher emissions than SOEC at any given carbon intensity due to its greater specific energy consumption. As shown in Fig. 15, the carbon intensity thresholds at which PEMEC and SOEC have lower specific emissions compared to SMR are 200 and 260 gCO_2/kWh, respectively.

Although the carbon intensity of grid electricity is decreasing in many European countries, it remains above the necessary threshold values in several regions. In these areas, fossil-based hydrogen production (via SMR) would currently result in lower CO_2 emissions compared to grid-powered electrolytic hydrogen production. To avoid the use of fossil-based electricity to power electrolysers, European Union has enacted, in 2023, a new amendment of the Renewable Energy Directive, referred to as RED III [70]. Among other matters, it sets strict requirements for the production of ammonia, both used as fuel or for industrial uses. To be accounted as Renewable Fuel of Non-Biological Origin (RFNBO), ammonia has to be produced exploiting electricity or from a renewable power plant directly connected to the HB plant, or bought through a Power Purchase Agreement (PPA) from a renewable power provider connected to the grid [71,72]. In case ammonia is not used as fuel but it has other industrial purposes (e.g. fertilisers production), RED III imposes that at least 42% of the used hydrogen must be RFNBO by 2030 [70]. This limit imposes the need for PPAs to cover at least 42% of the electricity used, in order to guarantee the conditions of temporal and geographical correlation as defined in RED III.

4. Conclusions

This study presents an economic and CO_2 emissions comparison of different ammonia production plants. The investigated layouts include three hydrogen production systems: steam methane reforming (SMR), low-temperature electrolysis (PEMEC), and high-temperature electrolysis (SOEC), including a deep thermal integration with the Haber-Bosch reactor. Although the methodology can be applied to various locations with minor changes in input parameters, this research focuses on the European context. Detailed process models of all plant sections are conducted to determine the Levelised Cost Of Ammonia (LCOA) for the three plants, including a sensitivity analysis on electricity and natural gas prices to assess their impact on the cost-competitiveness of these solutions. Beyond the economic analysis, direct and indirect CO_2 emissions are evaluated, encompassing direct emissions of SMR and indirect emissions associated with electricity and natural gas extraction and transport.

The main outcomes of the study can be summarised as follows:

- In the current scenario, SMR generally proves to be the most cost-effective solution due to the lower price of natural gas compared to electricity (in €/kWh), further emphasized by the high efficiency of the SMR process. Electrolysers become cost-competitive with SMR only if electricity prices fall below approximately 0.08 €/kWh_e: PEMEC becomes effective at an unrealistically low price of about 0.02 €/kWh_e, while SOEC is more economically viable at higher electricity prices (0.04–0.08 €/kWh_e) due to its superior efficiency. Given the current electricity and gas prices, significantly higher carbon taxes than the present levels are generally necessary to achieve cost parity between SMR and electrolysis.
- Electrolysers are expected to improve in terms of cost and performance in the coming years, potentially becoming more competitive with SMR at higher electricity prices. In the scenarios analysed for 2030 and 2040, SOEC (due to reductions in CAPEX) is projected to be more advantageous than PEMEC across all electricity prices. The electricity price range for the transition from SOEC to SMR is expected to be around 0.08–0.10 €/kWh_e in 2030 and 0.10–0.12 €/kWh_e in 2040. This range could increase further if carbon taxes on SMR emissions rise.
- The carbon footprint of electrolytic hydrogen – unlike that of SMR – heavily depends on the carbon intensity of the electricity used. Assuming grid power usage (without green power purchase agreement), SMR would remain the solution with lowest carbon emissions in many European countries where power production is still predominantly fossil-based. This set the need for tailored measures (such as RED III), to push ammonia toward a greener production, integrating it with renewable energy sources.

Overall, the sensitivity analyses presented in this study enable a rapid evaluation of the levelised cost of ammonia based on varying electricity and gas prices, along with an estimation of the associated CO_2 emissions. Future studies will focus on integrating ammonia production facilities with renewable power plants to achieve optimal design and operational strategies aimed at minimising both costs and emissions.

Acronyms

AEC	Alkaline Electrolyser Cell
ASU	Air Separation Unit
BOP	Balance Of Plant
CAPEX	Capital Expenditure
CO_2	Carbon Dioxide
ETS	Emissions Trading System
GHG	Greenhouse Gas
H_2	Hydrogen
HB	Haber-Bosch
HPC	High Pressure Column
HT WGS	High Temperature Water Gas Shift
LCOA	Levelised Cost Of Ammonia
LPC	Low Pressure Column
LT WGS	Low Temperature Water Gas Shift
M&R	Maintenance and Repair
NG	Natural Gas
NH_3	Ammonia
PEMEC	Proton Exchange Membrane Electrolyser Cell
PPA	Power Purchase Agreement
PSA	Pressure Swing Adsorption
RED	Renewable Energy Directive
RFNBO	Renewable Fuel of Non-Biological Origin
SE	Specific Emissions
SEC	Specific Electricity Consumption
SHC	Specific Heat Consumption
SMR	Steam Methane Reforming
SOEC	Solid Oxide Electrolyser Cell
WGS	Water Gas Shift

Declaration of generative AI and AI-assisted technologies in the writing process

During the preparation of this work the authors used ChatGPT-4 in order to improve the readability of the manuscript. After using this tool, the authors reviewed and edited the content as needed and take full responsibility for the content of the publication.

CRediT authorship contribution statement

Alessandro Magnino: Writing – original draft, Visualization, Software, Resources, Methodology, Investigation, Formal analysis, Data curation, Conceptualization. **Paolo Marocco:** Writing – review & editing, Visualization, Validation, Supervision, Project administration, Conceptualization. **Massimo Santarelli:** Writing – review & editing, Supervision. **Marta Gandiglio:** Writing – review & editing, Visualization, Validation, Supervision, Project administration, Funding

acquisition, Conceptualization.

Declaration of competing interest

The authors declare that they have no known competing financial interests or personal relationships that could have appeared to influence the work reported in this paper.

Acknowledgements

The work has been conducted in the framework of the AMPS (Automated Mass Production of SOC Stack) project (https://www.amps-project.eu/). The project is supported by the Clean Hydrogen Partnership and its members (GA: 101111882).

Project funded under the National Recovery and Resilience Plan (NRRP), Mission 4. Component 2 Investment 1.3 - Call for tender No. 1561 of 11.10.2022 of Ministero dell'Università e della Ricerca (MUR); funded by the European Union – NextGenerationEU. Project code PE0000021, Concession Decree No. 1561 of 11.10.2022 adopted by Ministero dell'Università e della Ricerca (MUR), CUP - E13C22001890001, Project title "Network 4 Energy Sustainable Transition – NEST".

Supplementary materials

Supplementary material associated with this article can be found, in the online version, at doi:10.1016/j.adapen.2024.100204.

Data availability

Data will be made available on request.

References

[1] United Nations. The Paris Agreement | UNFCCC 2016. https://unfccc.int/process-and-meetings/the-paris-agreement (accessed June 19, 2024).
[2] IPCC. Climate Change 2022 - Mitigation of Climate Change: Working. Group iii contribution to the sixth assessment report of the intergovernmental panel on climate change. Cambridge University Press; 2023. https://doi.org/10.1017/9781009157926.
[3] IRENA, AEA. Innovation outlook: renewable ammonia. 2022. https://www.irena.org/publications/2022/May/Innovation-Outlook-Renewable-Ammonia.
[4] European Hydrogen Observatory. The European hydrogen market landscape. 2023. https://observatory.clean-hydrogen.europa.eu/.
[5] Gabrielli P, Rosa L, Gazzani M, Meys R, Bardow A, Mazzotti M, et al. Net-zero emissions chemical industry in a world of limited resources. One Earth 2023;6:682–704. https://doi.org/10.1016/J.ONEEAR.2023.05.006.
[6] Statista. Ammonia production worldwide 2023 | Statista 2024. https://www.statista.com/statistics/1266378/global-ammonia-production/ (accessed June 19, 2024).
[7] Statista. Global ammonia demand value 2021-2050 | Statista 2024. https://www.statista.com/statistics/1345797/forecast-global-ammonia-demand-by-application/ (accessed June 19, 2024).
[8] Kurien C, Mittal M. Review on the production and utilization of green ammonia as an alternate fuel in dual-fuel compression ignition engines. Energy Convers Manag 2022;251:114990. https://doi.org/10.1016/J.ENCONMAN.2021.114990.
[9] Aziz M, TriWijayanta A, Nandiyanto ABD. Ammonia as effective hydrogen storage: a review on production, storage and utilization. Energies 2020;Vol 13:3062. https://doi.org/10.3390/EN13123062. Page 3062 202013.
[10] Rathore SS, Biswas S, Fini D, Kulkarni AP, Giddey S. Direct ammonia solid-oxide fuel cells: a review of progress and prospects. Int J Hydrogen Energy 2021;46:35365–84. https://doi.org/10.1016/J.IJHYDENE.2021.08.092.
[11] Zumdahl SS. Ammonia. Encycl Br.. 2024. https://www.britannica.com/science/ammonia.
[12] Kong H, Sun Y, Wang H, Wang J, Sun L, Shen J. Life cycle assessment of ammonia co-firing power plants: a comprehensive review and analysis from a whole industrial chain perspective. Adv Appl Energy 2024;14:100178. https://doi.org/10.1016/J.ADAPEN.2024.100178.
[13] Klerke A, Christensen CH, Nørskov JK, Vegge T. Ammonia for hydrogen storage: challenges and opportunities. J Mater Chem 2008;18:2304–10. https://doi.org/10.1039/b720020j.
[14] International Energy Agency. Ammonia technology roadmap. Paris; 2021. https://www.iea.org/reports/ammonia-technology-roadmap.
[15] Suryanto BHR, Matuszek K, Choi J, Hodgetts RY, Du HL, Bakker JM, et al. Nitrogen reduction to ammonia at high efficiency and rates based on a phosphonium proton shuttle. Science (80-) 2021;372:1187–91. https://doi.org/10.1126/SCIENCE.ABG2371.
[16] Soloveichik G. Electrochemical synthesis of ammonia as a potential alternative to the Haber–Bosch process. Nat Catal 2019;25:377–80. https://doi.org/10.1038/s41929-019-0280-0. 20192.
[17] Du H-L, Chatti M, Hodgetts RY, Cherepanov PV, Nguyen CK, Matuszek K, et al. Electroreduction of nitrogen with almost 100% current-to-ammonia efficiency. | Nat | 2022;609. https://doi.org/10.1038/s41586-022-05108-y.
[18] Mayer P, Ramirez A, Pezzella G, Winter B, Sarathy SM, Gascon J, et al. Blue and green ammonia production: a techno-economic and life cycle assessment perspective. IScience 2023;26:107389. https://doi.org/10.1016/J.ISCI.2023.107389.
[19] Weimann L, Gabrielli P, Boldrini A, Kramer GJ, Gazzani M. Optimal hydrogen production in a wind-dominated zero-emission energy system. Adv Appl Energy 2021;3:100032. https://doi.org/10.1016/J.ADAPEN.2021.100032.
[20] Nejadian MM, Ahmadi P, Houshfar E. Comparative optimization study of three novel integrated hydrogen production systems with SOEC, PEM, and alkaline electrolyzer. Fuel 2022. https://doi.org/10.1016/j.fuel.2022.126835.
[21] Ferrero D, Lanzini A, Santarelli M, Leone P. A comparative assessment on hydrogen production from low- and high-temperature electrolysis. Int J Hydrogen Energy 2013;38:3523–36. https://doi.org/10.1016/J.IJHYDENE.2013.01.065.
[22] Simpson AP, Lutz AE. Exergy analysis of hydrogen production via steam methane reforming. Int J Hydrogen Energy 2007;32:4811–20. https://doi.org/10.1016/J.IJHYDENE.2007.08.025.
[23] Nami H, Hendriksen PV, Frandsen HL. Green ammonia production using current and emerging electrolysis technologies. Renew Sustain Energy Rev 2024;199:114517. https://doi.org/10.1016/j.rser.2024.114517.
[24] Mersch M., Sunny N., Dejan R., Ku A.Y., Wilson G., O'reilly S., et al. A comparative techno-economic assessment of blue, green, and hybrid ammonia production in the United States 2024. https://doi.org/10.1039/d3se01421e.
[25] Zhang H, Wang L, Van herle J, Maréchal F, Desideri U. Techno-economic comparison of green ammonia production processes. Appl Energy 2020;259:114135. https://doi.org/10.1016/J.APENERGY.2019.114135.
[26] Campion N, Nami H, Swisher PR, Vang Hendriksen P, Münster M. Techno-economic assessment of green ammonia production with different wind and solar potentials. Renew Sustain Energy Rev 2023;173:113057. https://doi.org/10.1016/J.RSER.2022.113057.
[27] Sousa J, Waiblinger W, Friedrich KA. Techno-economic study of an electrolysis-based green ammonia production plant. Ind Eng Chem Res 2022;61:14515–30. https://doi.org/10.1021/ACS.IECR.2C00383.
[28] Kakavand A, Sayadi S, Tsatsaronis G, Behbahaninia A. Techno-economic assessment of green hydrogen and ammonia production from wind and solar energy in Iran. Int J Hydrogen Energy 2023;48:14170–91. https://doi.org/10.1016/J.IJHYDENE.2022.12.285.
[29] Lee B, Lim D, Lee H, Lim H. Which water electrolysis technology is appropriate?: critical insights of potential water electrolysis for green ammonia production. Renew Sustain Energy Rev 2021;143:110963. https://doi.org/10.1016/J.RSER.2021.110963.
[30] Bicer Y, Dincer I. Life cycle assessment of nuclear-based hydrogen and ammonia production options: a comparative evaluation. Int J Hydrogen Energy 2017;42:21559–70. https://doi.org/10.1016/J.IJHYDENE.2017.02.002.
[31] Egerer J, Grimm V, Niazmand K, Runge P. The economics of global green ammonia trade – "Shipping Australian wind and sunshine to Germany. Appl Energy 2023;334:120662. https://doi.org/10.1016/J.APENERGY.2023.120662.
[32] Ikaheimo J, Kiviluoma J, Weiss R, Holttinen H. Power-to-ammonia in future North European 100 % renewable power and heat system. Int J Hydrogen Energy 2018. https://doi.org/10.1016/j.ijhydene.2018.06.121.
[33] Eurostat. Statistics | Eurostat. Electricity prices for non-household consumers 2024. https://ec.europa.eu/eurostat/databrowser/view/nrg_pc_205/default/table?lang=en (accessed July 16, 2024).
[34] Eurostat. Statistics | Eurostat. Gas prices for non-household consumers 2024. https://ec.europa.eu/eurostat/databrowser/view/nrg_pc_203/default/table?lang=en (accessed July 16, 2024).
[35] European Commission. EU emissions trading system (EU ETS) - European Commission. 2024. https://climate.ec.europa.eu/eu-action/eu-emissions-trading-system-eu-ets_en. accessed July 15, 2024.
[36] Ember. Daily European Union Emission Trading System (EU-ETS) carbon pricing from 2022 to 2024 2024. https://www.statista.com/statistics/1322214/carbon-prices-european-union-emission-trading-scheme/.
[37] Antzara A, Heracleous E, Bukur DB, Lemonidou AA. Thermodynamic analysis of hydrogen production via chemical looping steam methane reforming coupled with in situ CO2 capture. Int J Greenh Gas Control 2015;32:115–28. https://doi.org/10.1016/J.IJGGC.2014.11.010.
[38] Katebah M, Al-Rawashdeh M, Linke P. Analysis of hydrogen production costs in Steam-Methane Reforming considering integration with electrolysis and CO2 capture. Clean Eng Technol 2022. https://doi.org/10.1016/j.clet.2022.100552.
[39] Voldsund M, Jordal K, Anantharaman R. Hydrogen production with CO2 capture. Int J Hydrogen Energy 2016;41:4969–92. https://doi.org/10.1016/J.IJHYDENE.2016.01.009.
[40] Lee S, Kim HS, Park J, Kang BM, Cho CH, Lim H, et al. Scenario-based techno-economic analysis of steam methane reforming process for hydrogen production. Appl Sci 2021;11:6021. https://doi.org/10.3390/APP11136021/S1.
[41] Crespi E, Guandalini G, Mastropasqua L, Campanari S, Brouwer J. Experimental and theoretical evaluation of a 60 kW PEM electrolysis system for flexible dynamic operation. Energy Convers Manag 2023;277:116622. https://doi.org/10.1016/J.ENCONMAN.2022.116622.

[42] Yodwong B, Guilbert D, Phattanasak M, Kaewmanee W, Hinaje M, Vitale G. Faraday's efficiency modeling of a proton exchange membrane electrolyzer based on experimental data. Energies 2020;13:1–14. https://doi.org/10.3390/en13184792.
[43] Mancera JJC, Manzano FS, Andújar JM, Vivas FJ, Calderón AJ. An optimized balance of plant for a medium-size PEM electrolyzer: design, control and physical implementation. Electron 2020;Vol 9:871. https://doi.org/10.3390/ELECTRONICS9050871. Page 871 20209.
[44] Murdoch H, Munster J, Satyapal S, Rustagi N, Elgowainy A, Penev M. Pathways to commercial liftoff. Clean Hydrogen. 2023. https://liftoff.energy.gov/wp-content/uploads/2023/03/20230320-Liftoff-Clean-H2-vPUB.pdf.
[45] Marocco P, Ferrero D, Lanzini A, Santarelli M. Optimal design of stand-alone solutions based on RES + hydrogen storage feeding off-grid communities. Energy Convers Manag 2021;238:114147. https://doi.org/10.1016/j.enconman.2021.114147.
[46] Crespi E, Guandalini G, Mastropasqua L, Campanari S, Brouwer J. Experimental and theoretical evaluation of a 60 kW PEM electrolysis system for flexible dynamic operation. Energy Convers Manag 2023;277:116622. https://doi.org/10.1016/j.enconman.2022.116622.
[47] Hauch A, Ploner A, Pylpko S, Mougin J, Cubizolles G. Test and characterization of reversible solid oxide cells and stacks for innovative renewable energy storage. 14th Eur. SOFC SOE Forum 2020:2020.
[48] Tian Y., Abhishek N., Yang C., Yang R., Choi S., Chi B., et al. Progress and potential for symmetrical solid oxide electrolysis cells 2022. https://doi.org/10.1016/j.matt.2021.11.013.
[49] Zhao Y, Xue H, Jin X, Xiong B, Liu R, Peng Y, et al. System level heat integration and efficiency analysis of hydrogen production process based on solid oxide electrolysis cells. Int J Hydrogen Energy 2021;46:38163–74. https://doi.org/10.1016/j.ijhydene.2021.09.105.
[50] Wang F, Wang L, Ou Y, Lei X, Yuan J, Liu X, et al. Thermodynamic analysis of solid oxide electrolyzer integration with engine waste heat recovery for hydrogen production. Case Stud Therm Eng 2021;27:101240. https://doi.org/10.1016/J.CSITE.2021.101240.
[51] Böhm H, Zauner A, Rosenfeld DC, Tichler R. Projecting cost development for future large-scale power-to-gas implementations by scaling effects. Appl Energy 2020;264:114780. https://doi.org/10.1016/j.apenergy.2020.114780.
[52] Nami H, Rizvandi OB, Chatzichristodoulou C, Hendriksen PV, Frandsen HL. Techno-economic analysis of current and emerging electrolysis technologies for green hydrogen production. Energy Convers Manag 2022;269:116162. https://doi.org/10.1016/J.ENCONMAN.2022.116162.
[53] Tsiklios C, Schneider S, Hermesmann M, Müller TE. Efficiency and optimal load capacity of E-fuel-based energy storage systems. Adv Appl Energy 2023;10:100140. https://doi.org/10.1016/J.ADAPEN.2023.100140.
[54] Yoshida M, Ogawa T, Imamura Y, Ishihara KN. Economies of scale in ammonia synthesis loops embedded with iron- and ruthenium-based catalysts. Int J Hydrogen Energy 2021;46:28840–54. https://doi.org/10.1016/j.ijhydene.2020.12.081.
[55] Cheng M, Verma P, Yang Z, Axelbaum RL. Flexible cryogenic air separation unit - an application for low-carbon fossil-fuel plants. Sep Purif Technol 2022;302:1383–5866. https://doi.org/10.1016/j.seppur.2022.122086.
[56] Agrawal R, Herron DM. Air liquefaction: distillation. Encycl Sep Sci 2000:1895–910. https://doi.org/10.1016/B0-12-226770-2/04821-3.
[57] Wu Y, Xiang Y, Cai L, Liu H, Liang Y. Optimization of a novel cryogenic air separation process based on cold energy recovery of LNG with exergoeconomic analysis. J Clean Prod 2020;275:123027. https://doi.org/10.1016/J.JCLEPRO.2020.123027.
[58] Wang C, Walsh SDC, Longden T, Palmer G, Lutalo I, Dargaville R. Optimising renewable generation configurations of off-grid green ammonia production systems considering Haber-Bosch flexibility. Energy Convers Manag 2023;280:116790. https://doi.org/10.1016/j.enconman.2023.116790.
[59] Armijo J, Philibert C. Flexible production of green hydrogen and ammonia from variable solar and wind energy: case study of Chile and Argentina. Int J Greenh Gas Control 2019. https://doi.org/10.1016/j.ijhydene.2019.11.028.
[60] Salvini C. Techno-economic analysis of small size second generation caes system. Energy Procedia 2015:782–8. https://doi.org/10.1016/j.egypro.2015.11.812.
[61] Wang K, Feng Y, Xiao F, Zhang T, Wang Z, Ye F, et al. Operando analysis of through-plane interlayer temperatures in the PEM electrolyzer cell under various operating conditions. Appl Energy 2023;348:121588. https://doi.org/10.1016/J.APENERGY.2023.121588.
[62] Skone TJ. Life cycle analysis of natural gas extraction and power generation office of fossil energy. National Energy Technology Laboratory (NETL); 2010. https://bit.ly/4fGAR7y.
[63] Schwietzke S, Griffin WM, Matthews HS, Bruhwiler LMP. Natural gas fugitive emissions rates constrained by global atmospheric methane and ethane. Environ Sci Technol 2014;48:7714–22. https://doi.org/10.1021/ES501204C.
[64] International Energy Agency. Methane tracker 2021. Paris; 2021. https://www.iea.org/reports/methane-tracker-2021.
[65] Eurostat. Database - Eurostat. 2024. https://ec.europa.eu/eurostat/data/database. accessed July 11, 2024.
[66] Statista. Natural gas commodity prices in Europe and the United States from 1980 to 2023, with a forecast for 2024 and 2025 2024. https://www.statista.com/statistics/252791/natural-gas-prices/ (accessed July 11, 2024).
[67] Electricity Maps. Electricity Maps | Emissioni di CO_2 in tempo reale del consumo elettrico 2024. https://app.electricitymaps.com/map?lang=it (accessed July 12, 2024).
[68] European Environment Agency. Greenhouse gas emission intensity of electricity generation 2024. https://www.eea.europa.eu/en/analysis/maps-and-charts/co2-emission-intensity-15 (accessed November 28, 2024).
[69] European Commission. 2040 climate target 2024. https://climate.ec.europa.eu/eu-action/climate-strategies-targets/2040-climate-target_en (accessed November 28, 2024).
[70] European Parliament. Directive (EU) 2023/2413 2023. http://data.europa.eu/eli/dir/2023/2413/oj.
[71] European Commission. Commission delegated regulation (EU) 2023/1184 2023. http://data.europa.eu/eli/reg_del/2023/1184/oj.
[72] Pexapark. European ppa market outlook 2024. 2024. https://pexapark.com/european-ppa-market/.